Extraction of Instantaneous and RMS Sinusoidal Jitter Using an Analytic Signal Method

Takahiro J. Yamaguchi, *Member, IEEE*, Mani Soma, *Fellow, IEEE*, Masahiro Ishida, Toshifumi Watanabe, and Tadahiro Ohmi, *Senior Member, IEEE*

***Abstract*—This paper describes a new method for extracting both instantaneous and rms sinusoidal jitter from phase-locked loops (PLL) output signals. The method is based on analytic signal theory and utilizes the Hilbert transform to extract phase information from a PLL signal. Both the theoretical basis and fundamental concepts of the new method are explained. A unified review of conventional methods is also presented. Results of Matlab simulations validate the performance of the new method for measuring jitter, and it is further validated by comparing experimental sinusoidal jitter results with those of a time interval analyzer.**

***Index Terms*—Analytic signal, Hilbert transform, oscilloscope, phase detector, phase noise, period jitter, PLL, sinusoidal jitter, timing interval analyzer, timing jitter, VCO, zero-crossing detector.**

I. Introduction and Problem Statement

JITTER of phase-locked loops (PLLs) is a fundamental limitation in high-speed digital communication systems and high-speed computer circuits. In communication systems, large jitter in the outputs of clock recovery circuits could easily result in data loss during data transmission. In high-speed computer circuits, large clock skews mandate slower computer operations in order to avoid errors. The measurement of jitter, both rms and peak-to-peak values, is extremely important since the measured values dictate the frequency performance of these systems. Moreover, since the recovered clock suffers from input-dependent jitter [1], in order to properly measure the jitter transfer function of transmission systems, calibration of the input sinusoidal jitter in terms of both peak-to-peak and rms values is required [2].

The PLL literature is replete with designs, analyzes (see e.g., [3]), and noise models for estimating jitter [4], [5]. Several papers presented at the recent International Test Conference proposed new methods to measure the jitter transfer function [6] and to generate tests for PLLs [7]. In these previous works, a threshold method is used to measure jitter, from which the jitter transfer function and bit error rate (BER) are inferred.

Manuscript received November 25, 2000; revised July 25, 2002. An earlierversion of this paper was presented at the IEEE VLSI Test Symposium, May 2000, Montreal, Canada. This paper was recommended by Associate Editor P. Mole.

T. J. Yamaguchi and M. Ishida are with the Advantest Laboratories, Ltd., Kamiayashi, Aoba-ku, Sendai, Miyagi, 989-3124, Japan (e-mail: jamax@atl.advantest.co.jp).

M. Soma is with the Department of Electrical Engineering, University of Washington, Seattle, WA 98195 USA.

T. Watanabe is with the Advantest Corporation, Ora, Gunma 370-0718, Japan.

T. Ohmi is with the New Industry Creation Hatchery Center, Tohoku University, Sendai 980-8579, Japan.

Digital Object Identifier 10.1109/TCSII.2003.812916

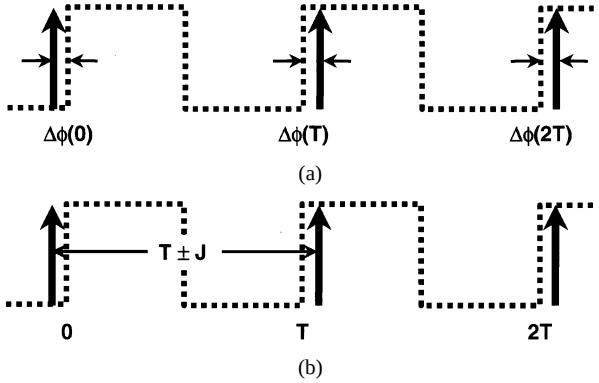

Fig. 1. Timing jitter and period jitter. (a) Timing jitter. (b) Period jitter.

These methods are only tangentially related to the focus of this paper. PLL jitter measurement methods are not new, of course. Several methods have been implemented in test systems, as reviewed in Section II below.

The method presented here relies on frequency-domain analysis of the clock waveform, which differs from conventional time-domain methods. Conventional time-domain methods estimate the locations of the edges of the real clock signal and extract period jitters from these edges. In contrast, this method, which is based on the Hilbert transform, estimates the instantaneous phase from a complex clock signal, and the ideal linear phase component from the slope of a straight-line fit to the phase. The difference between the phase and the ideal linear phase component is the instantaneous phase noise, which corresponds to the timing jitter values at the zero-crossings.

It will be shown that this method has comparable accuracy to existing methods, but requires a much smaller number of signal samples (hence is faster), and can be implemented at lower cost.

In this paper, Section III presents the theoretical basis of the proposed method for extracting both rms and peak-to-peak timing jitter values. Section IV describes the jitter extraction procedure and considers the relationship between timing jitter and period jitter for sinusoidal jitter measurements. In Section V, jitter is estimated from a random input source using the new method and the results are compared with those of other methods. In Section VI, the proposed method is validated for measuring sinusoidal jitter by comparing its results with the expected results of a controlled experiment.

II. Existing Jitter Measurement Methods

In this paper, jitter will be classified as either ***timing jitter*** or ***period jitter***. Fig. 1(a) illustrates ***timing jitter*** $\Delta\phi(nT)$ (in radians). This is the deviation of rising edges from integer

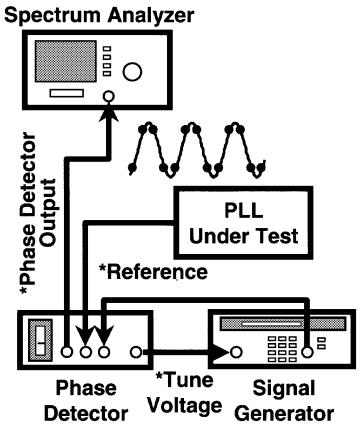

Fig. 2. Test setup for measuring phase noise using the phase detector method.

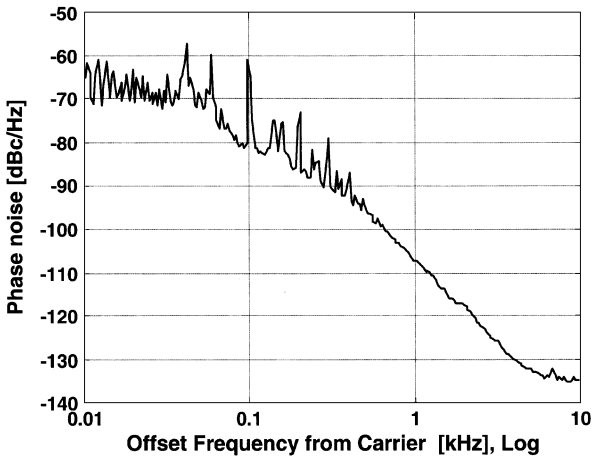

Fig. 3. Typical phase noise measurement using the phase detector method.

multiples of the pulse repetition period (nT). In order to show its discrete-time property, we will use the notation $\Delta\phi[n]$ $(= \Delta\phi(nT))$. The continuous function $\Delta\phi(t)$ is sometimes referred to as ***phase noise***, or instantaneous phase noise.

The term ***period jitter***, frequently referred to simply as ***jitter*** in digital systems, is used to describe the period fluctuation. This jitter [shown in Fig. 1(b)] will be denoted by J. It is related to the timing jitter of square wave edges or zero crossings by the equations:

$$J[n] = \Delta\phi[n+1] - \Delta\phi[n] \text{ [radian]} \quad (1)$$

$$J[n] = \frac{\Delta\phi[n+1] - \Delta\phi[n]}{\frac{2\pi}{T}} \text{ [s]}. \quad (2)$$

The two most popular (traditional) methods for measuring PLL jitter are as follows.

- **Phase Noise Measurement:** The rms values of phase noise are measured by combining a phase detector with a spectrum analyzer, or by using a sampler-based Hilbert method.
- **RMS and Peak-to-Peak Period Jitter Measurement:** The rms and peak-to-peak period jitter are measured using zero-crossing detectors. These methods include counter-based measurement, oscilloscope-based histogram measurement, and time-interval analyzer measurement.

These methods have been implemented in desktop measurement instruments. They will serve as benchmarks for comparison with our proposed method.

A. Phase Noise Measurement

Spectrum Analyzer (Phase Detector Method): A spectrum analyzer measures phase noise as a phase difference spectrum in the frequency domain. Fig. 2 shows a typical test setup. The output signal of the PLL under test and the reference sinusoid generated by a signal generator are fed into a phase detector. These two signals are maintained to be at the same frequency, but in "quadrature" (90 degrees out of phase) with each other. The phase detector provides the phase difference between these two signals. This phase difference signal is input to the spectrum analyzer, and the resulting phase noise spectrum is used for rms value extraction.

The mean-square value of phase noise is related to the area under the phase noise spectrum curve. The rms value of phase noise is given by the positive square root of the mean-square value.

This method treats jitter as an infinite number of phase modulation sideband frequencies extending above the PLL oscillation frequency, as shown in Fig. 3. While the measurement bandwidth of this method is wide, its throughput is low. For this example, it took 600 seconds (10 minutes) to perform the measurement.

This method has two major weaknesses. First, the peak-to-peak value of phase noise cannot be measured by this method. Secondly, if the phase noise of the reference sinusoid is not sufficiently small compared with that of the PLL under test, keeping two oscillators in quadrature is required.

Sampler-Based Measurement of Sinusoidal Jitter: Hewlett-Packard employs the Hilbert transform in its sampler-based jitter measurement instruments, e.g., the HP 71501B. Although our new method also uses the Hilbert transform, our use of it is quite different than its use by HP.

The HP method [8] first samples the input signal $x(t)$, and performs a Fast Fourier Transform (FFT) on the sampled data $x(t)$. This frequency spectrum then undergoes a Hilbert transform, and is then converted back to the time domain using the inverse FFT. This process yields the quadrature component $H[x(t)]$, which when combined with the original sampled data $x(t)$, provides the analytical signal to be used in estimating instantaneous phase noise. This technique has been applied to the measurement of the intrinsic jitter and the jitter transfer function in telecommunication systems.

B. Zero-Crossing Detector

The zero crossings of a PLL output signal provide a measure of the instantaneous period of oscillation. Consequently, period jitter can be measured by estimating the fluctuations in the time spacing between positive-going zero crossings. Fig. 4 illustrates an example of a square wave and its corresponding instantaneous period, plotted as functions of time.

The period was estimated using a zero-crossing detector. The zero-crossing detector will give good statistical estimates of period jitter only when there is no change in the period of a PLL

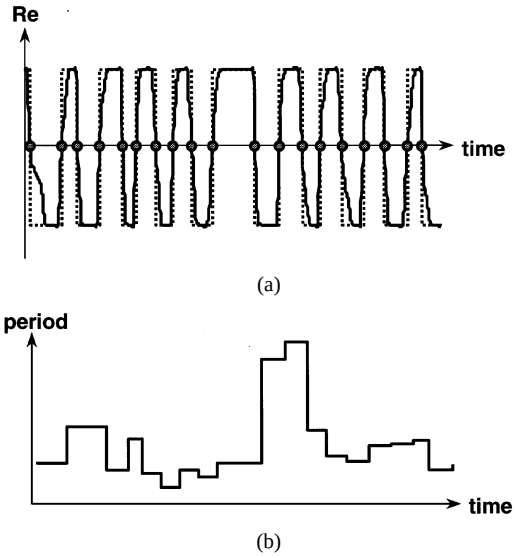

Fig. 4. Zero-crossing detector. (a) Square wave. (b) Instantaneous period estimated using the half period of the signal as a measuring interval.

output signal during the measurement. Otherwise, the statistical distribution of the period will spread more widely due to these variations in the period.

Counter-Based Measurement: The counter-based measurement method is rooted in the time-domain characterization of the frequency stability of certain frequency sources such as quartz-crystal oscillators and atomic frequency standards. This method uses a digital counter to count the number of internal reference clock pulses during the time interval between successive zero crossings of a PLL output signal. Time interpolation is also used to achieve better resolution than can be achieved from the normal round-off error imposed by the reference clock period. Statistical analysis is also used to extract jitter measurements with higher accuracy. However, the throughput of this method is low due to the large volume of data required for statistical validation.

Oscilloscope-Based Jitter Histogram Measurement: The oscilloscope-based histogram method determines the timing distribution of threshold crossings over a specific time window. This method requires a jitter-free triggering signal in order to capture the jittery signal. To make this measurement, a reference triggering edge, threshold values for high and low voltages, and the number of samples to be acquired must be pre-defined.

The histogram is then constructed by counting the number of samples that occur during a specific time/voltage window as illustrated in the right portion of Fig. 5. Jitter data is then extracted from this histogram.

A typical setup for sinusoidal jitter testing, a signal edge, and the jitter histogram are shown in Fig. 5. The histogram indicates rms and peak-to-peak values of 38.42 ps and 130 ps, respectively. For this example, it took 60 seconds to collect the 5000 samples required to construct the jitter histogram. The throughput of this method is obviously low due to the time required to collect the histogram data sample by sample, using a trigger.

Time Interval Analyzer: The time interval analyzer (TIA) measures the time interval between two adjacent zero-crossing

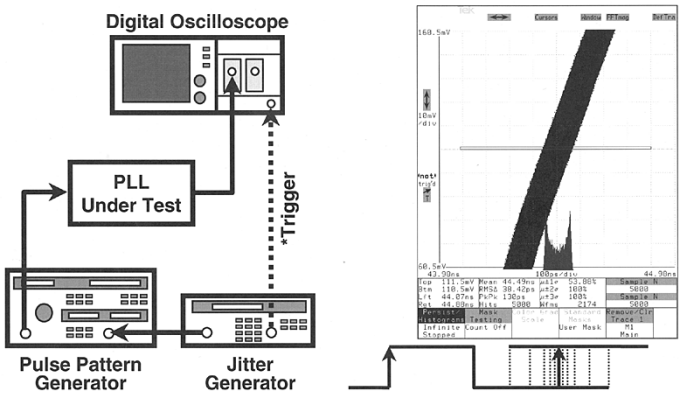

Fig. 5. Oscilloscope-based histogram jitter measurement. (The left rising edge at time $[0]$ is defined as the reference point by using the external trigger signal. The right edge rises at time $[1]+\Delta\phi[1]-\Delta\phi[0]$).

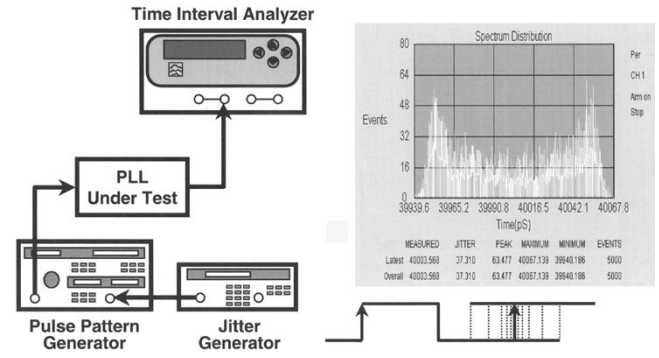

Fig. 6. Jitter histogram measurement using a time-interval analyzer. (The left rising edge at time $[0]$ is defined as the reference point by using the internal trigger signal. The right edge rises at time $[1]+\Delta\phi[1]-\Delta\phi[0]$).

events of a PLL output signal. It does this by reading time stamp values out of its own internal time-base counter. This method does not require a triggering signal. The construction of a statistical model for jitter using the measured interval as a random variable permits both rms and peak-to-peak jitter measurements with this method.

There are two ways to implement the TIA method. The first measures the jittery signal continuously using a zero-dead-time counter [9], and the other repeatedly measures jitter, but requires an intermediate 25-μs dead-time [10].

Since the zero-dead-time TIA records the time stamp associated with each sampled zero-crossing event [9], it can be used to measure timing jitter by estimating ideal zero-crossing timings using a least-squares curve fit to the phase progression data. Nevertheless, in Sections IV-B and VI-B, we will show that even a zero-dead-time measurement capability is insufficient to accurately estimate sinusoidal jitter.

Fig. 6 shows a typical setup and the resulting jitter histogram for sinusoidal jitter testing using the TIA method. The histogram indicates rms and peak-to-peak values of 37.31 ps and 127 ps, respectively. In this case it only took 2 seconds to collect the required 5000 samples. This compares favorably to the oscilloscope-based jitter histogram test result shown in Fig. 5, which took 30 times longer to make.

In zero crossing counting, sampling of the time stamp can be done at a rate slightly higher than the Nyquist sampling rate [9]. However, the time resolution of the internal time-base counter

must be increased as the input frequency increases or as the expected jitter values become small.

III. Analytic Signal Theory for Jitter Measurement

In this section, we describe the theoretical basis of our method for measuring both rms and peak-to-peak timing jitter values. It will be shown that this method has comparable accuracy to the existing methods previously reviewed, but requires a much smaller number of signal samples (hence is faster), and can be implemented at lower cost.

The method relies on the transformation of a real signal into an analytic signal by using the Hilbert transform. Our new method will be called the "$\Delta\phi$ method" since it relies on an instantaneous phase function to extract jitter.

A. Review of the Hilbert Transform

The Hilbert transform [11] of a time function $x_a(t)$ is defined by,

$$\hat{x}_a(t) = H[x_a(t)] = \frac{1}{\pi}\int_{-\infty}^{+\infty}\frac{x_a(\tau)}{t-\tau}d\tau. \tag{3}$$

Thus $\hat{x}_a(t)$ is the convolution of the functions $x_a(t)$ and $(1/\pi t)$. That is, the Hilbert transform is equivalent to passing $x_a(t)$ through an all-pass filter, in which the magnitudes of the spectral components are unchanged but their phases are shifted by 90 degrees $(\pi/2)$. The analytic signal $z(t)$ [11] associated with a real signal $x_a(t)$ is defined as the complex signal

$$z(t) \equiv x_a(t) + j\hat{x}_a(t) \tag{4}$$

where the imaginary part $\hat{x}_a(t)$ is the Hilbert transform of the real part $x_a(t)$. From this, we can define an instantaneous phase $\phi(t)$ of the real signal $x_a(t)$,

$$\phi(t) = \tan^{-1}\left[\frac{\hat{x}_a(t)}{x_a(t)}\right]. \tag{5}$$

It can be shown that the ***time rate of change*** of the phase of this analytic signal is exactly the instantaneous frequency [11]. This is a fundamental property to be exploited by our new method, which consequently has been named the $\Delta\phi$ method.

Since jitter can be modeled as phase modulation imposed on a perfect square wave, we will use the analytic signal generated by the Hilbert transform as the basis for extracting jitter values from a PLL output signal.

B. Extraction of Jitter From an Analytic Signal

To extract jitter values for a PLL, we will examine an analytic signal model for the input and output waveforms of the voltage-controlled oscillator (VCO) in the PLL. Fig. 7 shows the complex signal model of the VCO. Its input is a real-valued signal. Its output is reformulated as an analytic signal, where the real part is a cosine wave and the imaginary part is a sine wave. The $\Delta\phi$ method estimates the instantaneous phase using this analytic signal.

A jitter-free PLL output is a square wave of fundamental frequency f_0. This signal can be decomposed by Fourier analysis into a sum of sine harmonics of frequencies f_0, $3f_0$, $5f_0$, etc.

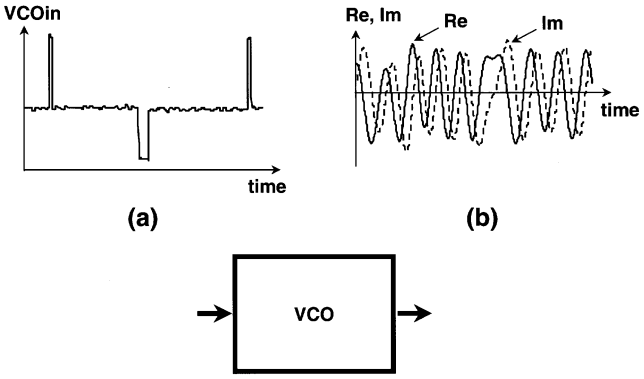

Fig. 7. Analytic signal model for VCO. (a) Input signal to the VCO. (b) Output signal from the VCO as an analytic signal.

When this signal is passed through a bandpass filter with center frequency at f_0, the fundamental component will have a period of $T = 1/f_0$. Due to the phase noise, the instantaneous phase deviates from integer multiples of T [Fig. 1(a)], and the deviation is measured as timing jitter.

With jitter added, the fundamental sinusoidal component with amplitude A and frequency f_0 can be written as:

$$A\cos(\phi(t)) = A\cos(2\pi f_0 t + \phi_0 - \Delta\phi(t)). \tag{6}$$

Notice that the total instantaneous phase function $\phi(t)$ has been written as the sum of 3 components:

- the linear phase component, which contains the fundamental frequency f_0;
- a constant phase component ϕ_0, which can be normalized to zero for computational convenience;
- the phase modulation component $-\Delta\phi(t)$, which is the timing jitter.

The analytic signal $z(t)$ corresponding to the signal in (6) is

$$z(t) = A\cos(2\pi f_0 t + \phi_0 - \Delta\phi(t)) + jA\sin(2\pi f_0 t + \phi_0 - \Delta\phi(t)). \tag{7}$$

This signal is a rotating phasor in the complex frequency domain. The amplitude of the phasor is A. If the values of both the real and imaginary parts are given at specific time points, it is quite simple to compute the instantaneous phase function $\phi(t)$ using (5). This phase modulation component can be extracted from sampled data. The values of the phase modulation at the zero crossings of the original clock waveform, $-\Delta\phi[n]$, are used to extract both the rms and peak-to-peak timing jitter simultaneously without requiring any extra measurements:

- $\Delta\phi[n] = \Delta\phi(t)$ at $t = nT$ where nT corresponds to the multiple times of the clock edges.
- The rms value of $\Delta\phi[n]$ is the rms timing jitter $\Delta\phi_{\mathrm{RMS}}$.
- The peak-to-peak timing jitter $\Delta\phi_{\mathrm{PP}}$ is calculated by the difference: $[\max\{\Delta\phi[n]\} - \min\{\Delta\phi[n]\}]$.

This is the essence of the $\Delta\phi$ method. Section IV describes it as an algorithm.

IV. Jitter Extraction by the $\Delta\phi$ Method

In this section, we first show how the $\Delta\phi$ method estimates both rms and peak-to-peak timing jitter values of a PLL output

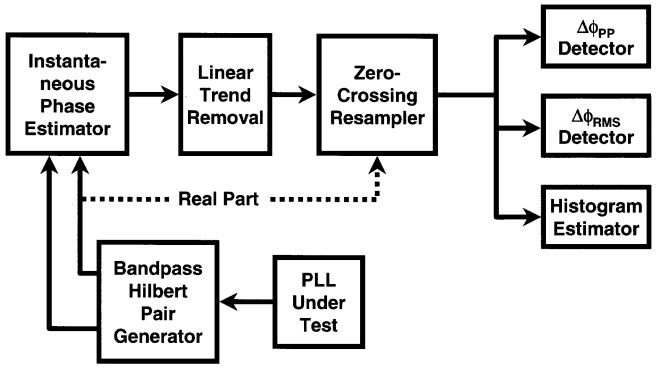

Fig. 8. Timing jitter extraction algorithm.

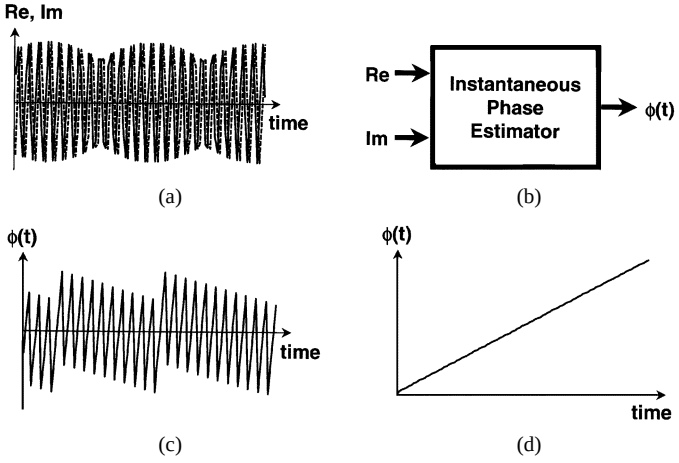

Fig. 9. Instantaneous phase estimator with representative input/output signals. (a) Input signals (analytic signal). (b) Instantaneous phase estimator block. (c) Instantaneous phase. (d) Output unwrapped phase.

signal. Also, differences between our method and the Hewlett-Packard method will be discussed.

A. Jitter Extraction Procedure

Fig. 8 illustrates the proposed algorithm for extracting timing jitter using the analytic signal method. The PLL output waveform is sampled using an analog-to-digital converter (ADC). The sampled PLL output is bandpass filtered to extract the signal with fundamental frequency f_0 and the Hilbert pair generator converts the signal to an analytic signal (both real and imaginary parts), as shown in Fig. 9(a). The instantaneous phase estimator [Fig. 9(b)] provides the instantaneous phase output shown in Fig. 9(c). The phase is unwrapped to remove 2π discontinuities as illustrated in Fig. 9(d).

Finally, the continuous phase is input to the linear trend removal block, shown in Fig. 10, which performs a least-squares fit of a straight line to $\phi(t)$. Then, the linear phase component $(2\pi f_0 t+\phi_0)$ is subtracted from $\phi(t)$. What remains is the phase noise $\Delta\phi(t)$ as function of time (Fig. 10(b))

$$\Delta\phi(t) = -\{\phi(t) - (2\pi f_0 t + \phi_0)\} \quad \text{(after straight line removal)}. \tag{8}$$

The linear phase component corresponds to a jitter-free signal. Note also that the *slope* of the best-fit straight line

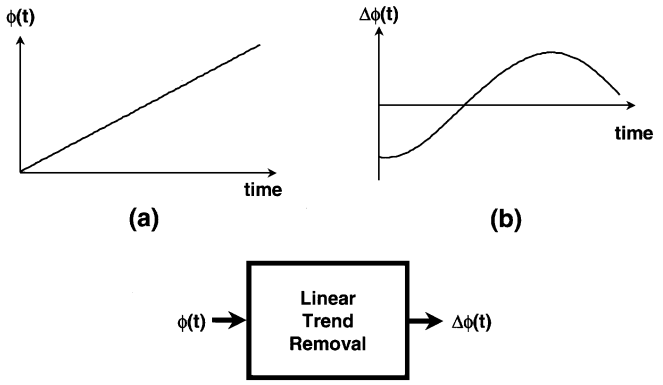

Fig. 10. Linear trend removal with representative input/output signals. (a) Unwrapped phase. (b) Instantaneous phase noise.

can be used to estimate the fundamental frequency f_0, thus providing another piece of data to verify the performance of the PLL.

Procedures for calculating the Hilbert transform and for obtaining a continuous phase function are discussed below.

Hilbert Transform: The Hilbert pair generator can be implemented on an ATE system in the following steps, using DSP tools [12].

1) Apply the fast Fourier transform (FFT) to the PLL output signal to obtain the two-sided spectrum (positive and negative frequencies).
2) Zero the negative frequency components of the spectrum.
3) Multiply the positive frequency components by two.
4) Apply the inverse FFT to the two-sided spectrum with zero negative frequencies. The result is a complex valued analytic function of the original signal.

Note that, in step 2, the bandpass filtering can also be accomplished by applying a rectangular filter centered at f_0 to the positive frequency components. Applying a rectangular filter before performing the inverse FFT reduces the computational requirement compared to performing bandpass filtering on the time-domain signal.

Frequency resolution of the measurement is inversely proportional to the record length of the signal $z(t)$. In order to achieve higher frequency resolution, long-time records $x_a(t)$ are partitioned into several smaller sets of samples, and a Hanning window is applied to each set of samples before the FFT is applied. This is a standard windowing procedure used to minimize errors when the FFT is applied to signals that are nonperiodic (not completely contained within) a set of time-domain samples [13].

By overlapping the adjacent sections of samples we can eliminate not only the end effects due to windowing and FFT [13] but also large errors associated with data points $z(t)$ due to the small values of window function and the inverse FFT. Therefore, segment overlapping can be used to generate a long-term analytic signal $z(t)$ with limited samples $x_a(t)$.

Continuous Phase Function: The instantaneous phase estimator outputs the instantaneous phase $\phi(t)$ shown in Fig. 9(c). This signal can be written as

$$\phi(t) = [2\pi f_0 t + \phi_0 - \Delta\phi(t)] \bmod 2\pi. \tag{9}$$

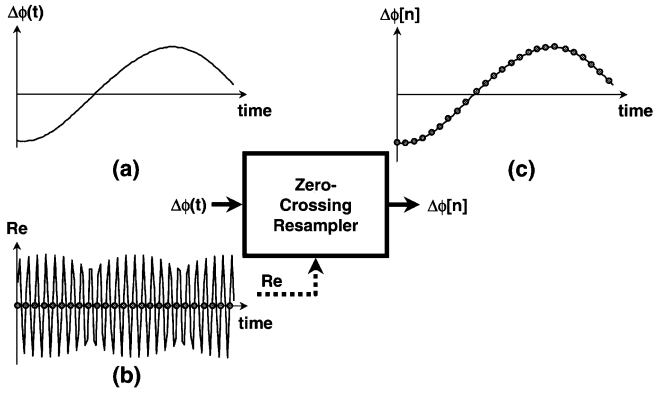

Fig. 11. Zero-crossing re-sampler with representative input/output signals. (a) Instantaneous phase noise. (b) Real part of the analytic signal. (c) Instantaneous phase noise re-sampled at its zero crossings.

$\phi(t)$ represents the principal value of the phase. Its values lie in the range $[-\pi, +\pi]$. Therefore, there exist discontinuity points at $-\pi$ and $+\pi$ as shown in Fig. 9(c). In order to convert the phase function to a continuous curve, it is unwrapped by appropriately adding multiples of 2π to the principal value $\phi(t)$ until all discontinuities are removed

$$\phi(t) = 2\pi f_0 t + \phi_0 - \Delta\phi(t) \tag{10}$$

Fig. 9(d) shows a continuous phase function $\phi(t)$ without discontinuities. Removing the linear component from this phase function produces the phase noise $\Delta\phi(t)$ as illustrated in Fig. 10.

Utilizing this phase noise, the $\Delta\phi$ method can estimate both the peak-to-peak and rms values of phase noise as shown below.

Phase Noise Values: The peak-to-peak value of phase noise is calculated from the $\Delta\phi(t)$ waveform:

$$d(\{\Delta\phi\}) = \max\{\Delta\phi(t)\} - \min\{\Delta\phi(t)\} \text{ [radian]}. \tag{11}$$

The rms value of phase noise is also computed from the same waveform:

$$\sigma_{\Delta\phi} = \sqrt{\frac{1}{M}\sum_{t=0}^{M-1}\Delta\phi^2(t)} \text{ [radian]} \tag{12}$$

where M is the number of ADC sampling points.

Next, the zero-crossing re-sampler is applied to the $\Delta\phi(t)$ waveform to re-sample it at its positive-going zero crossings $t = nT$

$$\Delta\phi[n] = \Delta\phi(t)|_{t=nT}. \tag{13}$$

This procedure is illustrated in Fig. 11. Note that zero crossings are easily determined from the real part of the analytic signal.

Timing Jitter Values: Since $\Delta\phi[n]$ is a timing jitter sequence, the peak-to-peak value of timing jitter is calculated from the $\Delta\phi[n]$ sequence:

$$\Delta\phi_{\mathrm{PP}} = \max\{\Delta\phi[n]\} - \min\{\Delta\phi[n]\} \text{ [radian]}. \tag{14}$$

The rms timing jitter is also directly computed from the same sequence:

$$\Delta\phi_{\mathrm{RMS}} = \sqrt{\frac{1}{N}\sum_{k=0}^{N-1}\Delta\phi^2[k]} \text{ [radian]} \tag{15}$$

where N is the number of the positive-going zero crossings. The algorithm description is now complete.

Several features of this algorithm should be emphasized:

- period jitter, timing jitter, and phase noise are extracted simultaneously;
- no histogram is required, so there is no need for extensive data collection to validate statistics.

Comparison With Hewlett Packard Method: Our technique uses the Hilbert transform, but differs from the Hewlett-Packard technique [8] in several aspects.

1) The original signal is bandpass filtered (windowed in the frequency domain) to isolate the fundamental frequency component.
2) The analytic signal is generated from the real and imaginary parts of the inverse Fourier transform of the two-sided spectrum, not by combining the quadrature component with the original sampled data. This reduces errors due to sampling and other nonlinear effects.
3) The Hewlett-Packard technique measures instantaneous phase, but not timing jitter or period jitter.

B. Relationship Between Timing Jitter and Period Jitter

RMS timing jitter $\Delta\phi_{\mathrm{RMS}}$ is the standard deviation of the timing accuracy. As explained in Section II-B, period jitter $J[m]$ is measured by comparing variances of adjacent zero crossings with each other. Thus J_{RMS} corresponds to the standard deviation of the difference of two correlated timing variables

$$\begin{aligned} J_{\mathrm{RMS}} &= \sqrt{\left\langle \{\Delta\phi[m+n] - \Delta\phi[m]\}^2 \right\rangle} \\ &= \sqrt{2(1-\rho(n))}\Delta\phi_{\mathrm{RMS}} \end{aligned} \tag{16}$$

where $\rho(n)$ is the correlation coefficient between $\Delta\phi[m+n]$ and $\Delta\phi[m]$ [12]. Note that, if $n =$ (complete half-period of the sine wave), $\Delta\phi[m+n]$ and $\Delta\phi[m]$ are always out of phase and so $\rho(n) = -1$. Thus, in this case J_{RMS} is equal to $2\Delta\phi_{\mathrm{RMS}}$. In general, jitter ratio (rms period jitter divided by rms timing jitter) falls between 0 and 1

$$\frac{J_{\mathrm{RMS}}}{2\Delta\phi_{\mathrm{RMS}}} = \sqrt{\frac{1-\rho(n)}{2}}. \tag{17}$$

This result is also verified in Section VI-A.

To verify the $\Delta\phi$ method by comparing estimated J_{RMS} and J_{PP} values with those measured using a conventional zero-crossing detector, we need to convert $\Delta\phi[m]$ to $J[m]$. Hence we will add a digital differentiator between the zero-crossing re-sampler and the $\Delta\phi_{\mathrm{PP}}/\Delta\phi_{\mathrm{RMS}}$/histogram estimators in the diagram shown in Fig. 8. The differentiator receives two samples $\Delta\phi[m]$ and $\Delta\phi[m+n]$ as inputs, and computes the jitter sequence $J[m]$ using (1) or (2).

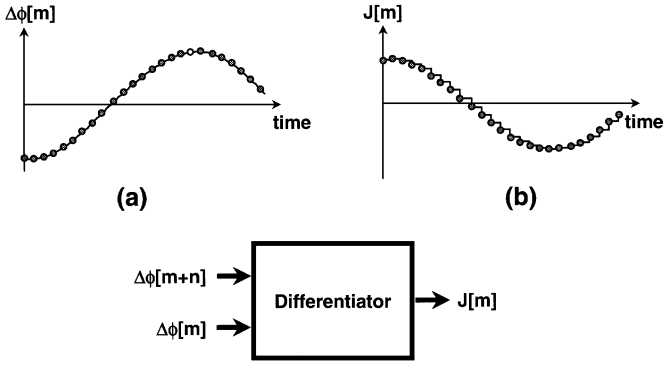

Fig. 12. Differentiator with representative input/output signals ($m = 0, 1, 2, \ldots$; $n = 17$ cycles). (a) Input to the differentiator. (b) Output from the differentiator using the $\Delta\phi$ method.

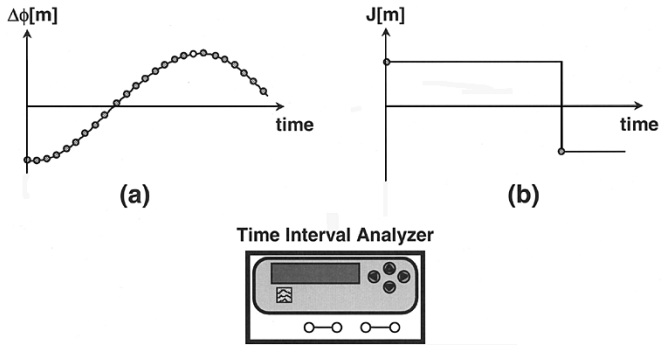

Fig. 13. Measurements using the TIA method: Less time resolution ($m = 0, 17, 34, \ldots$; $n = 17$ cycles). (a) Input to the differentiator. (b) Output from the differentiator using the TIA method.

Fig. 12 illustrates the typical input and output of the differentiator. By comparison, even the zero-dead-time jitter measurement performed with the TIA results in a poor time resolution estimation, as illustrated in Fig. 13. This coarse resolution results in noticeable error in the measurement of peak-to-peak jitter J_{PP}. This will be shown in Section VI-B.

V. Simulation and Experimental Results Using Random Noise

In this section, the performance of the proposed $\Delta\phi$ method is compared with the phase detector and zero-crossing detector methods. To simulate a noisy environment, a controlled experiment was implemented in Matlab, with additive noise injected into a VCO to create random jitter. The phase detector, zero-crossing detector, and $\Delta\phi$ method were also implemented as Matlab routines. The simulated results and comparisons are presented in Sections V-A and V-B below [14]. Section V-C shows the experimental results of the phase noise measurements.

A. RMS Phase Noise Comparison

As previously described, the phase detector method provides a good measure of rms phase noise with wide measurement bandwidth. A large number of controlled experiments were performed to compare this method with the $\Delta\phi$ method. In each experiment (with a sample size of 14 000), a different level of additive noise was injected into the VCO to generate jitter. The rms jitter value was measured by each method for each noise level.

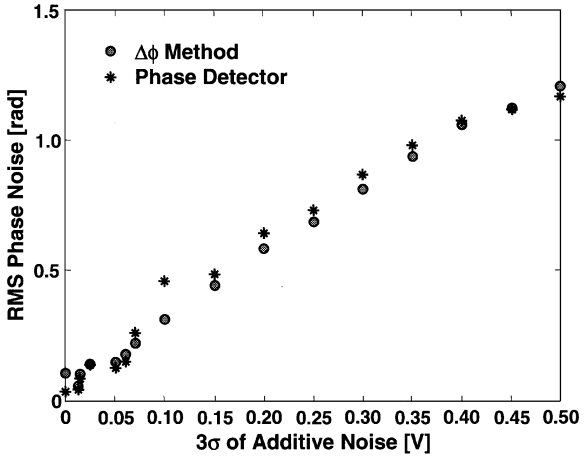

Fig. 14. RMS phase noise comparison for various noise levels.

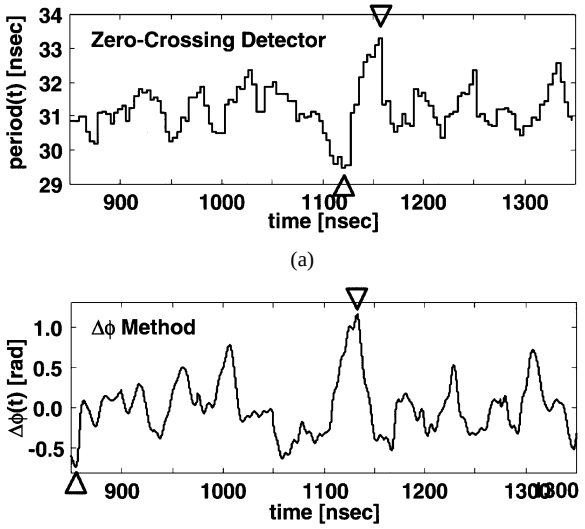

Fig. 15. Peak-to-peak value of instantaneous phase noise (marked by triangles) for one noise level. (a) Zero-crossing detector. (b) $\Delta\phi$ method.

Fig. 14 shows $\sigma_{\Delta\phi}$ values measured by both methods as the noise level (characterized by its root-mean-square) was increased from 0.0 to 0.5 V. The symbol "$*$" represents data computed by the phase detector method. The two sets of results show excellent agreement with each other. Because the $\Delta\phi$ method measures $\sigma_{\Delta\phi}$ without sweeping a bandpass filter over the band, it is 1000 times faster for the same amount of accuracy and measurement bandwidth. Moreover, the $\Delta\phi$ method does not require the time-consuming calibration of a phase detector constant [15].

B. Peak-to-Peak Phase Noise Comparison

For this comparison, peak-to-peak deviation values in the instantaneous period of the VCO output were estimated using both the TIA method (with a zero-dead-time counter) and the $\Delta\phi$ method. With one specific level of additive noise injected into the VCO, it is quite instructive to examine the zero-crossing detector output [shown in Fig. 15(a)] and the instantaneous phase

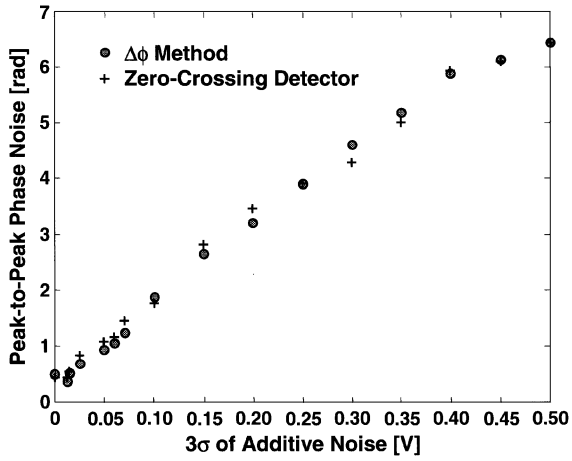

Fig. 16. Peak-to-peak phase noise comparison for various noise levels.

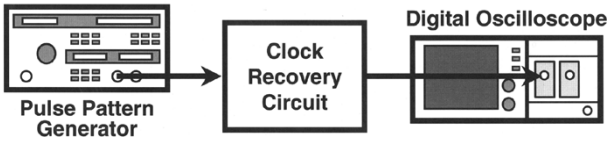

Fig. 17. Experimental setup for measring phase noise using the $\Delta\phi$ method.

noise $\Delta\phi(t)$ of the $\Delta\phi$ method [shown in Fig. 15(b)]. The instantaneous phase noise plot shows much finer time resolution than the TIA result. In other words, the $\Delta\phi$ method accurately observes $\Delta\phi(t)$, while only a coarse version of $\Delta\phi(nT)$ can be observed through the zero-crossing detector. Thus, the $\Delta\phi$ method is expected to provide much more accurate peak-to-peak phase noise estimation.

When the additive noise level is varied, the peak-to-peak phase noise extracted by both methods is almost identical, as shown in Fig. 16.

C. Experimental Phase Noise Measurement

RMS phase noise $(\sigma_{\Delta\phi})$ measurements between the $\Delta\phi$ method and the phase detector method (using a spectrum analyzer, Advantest R3267) were also compared. Fig. 17 shows the measurement setup. The pulse pattern generator (Advantest D3173) supplied a $2^{15} - 1$ pseudo-random bit sequence (PRBS) at 2.488 32 Gbps to a clock recovery circuit, which also includes an E/O (Electrical to Optical) converter, an O/E (Optical to Electrical) converter and a SAW filter. A recovered clock signal was digitized using an oscilloscope (Tektronix TDS694C with 8 bit ADC, $f_{\mathrm{SAMPLING}} = 10$ GHz, $\mathrm{bandwidth} = 3$ GHz). Fig. 18(a) shows a few cycles of this digitized recovered clock signal. Since the 3 dB bandwidth of the oscilloscope is 3 GHz, the second and third harmonics of the recovered clock signal were rejected. Therefore, in this case, the digitized recovered clock happened to be almost identical to the band limited waveform produced by bandpass filtering with a lower cutoff frequency $= (2.49\ \mathrm{GHz} - 20\ \mathrm{MHz})$ and an upper cutoff frequency $= (2.49\ \mathrm{GHz} + 20\ \mathrm{MHz})$. The bandlimited waveform is plotted in Fig. 18(b). The total number of samples for the entire experiment is 120 000.

The phase noise spectrum of the recovered clock signal (measured by the spectrum analyzer) is plotted in Fig. 19. The $\sigma_{\Delta\phi}$ value is 0.046 radians. Fig. 20(b) is the corresponding phase noise spectrum estimated by the $\Delta\phi$ method. It indicates a $\sigma_{\Delta\phi}$ value of 0.043 radians. Fig. 20(a) shows the instantaneous phase noise $\Delta\phi(t)$.

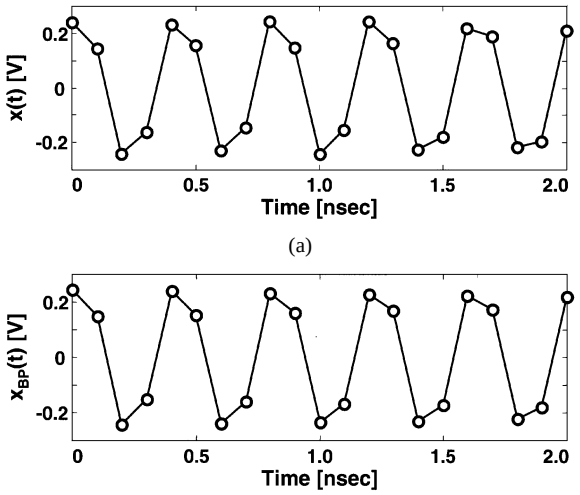

Fig. 18. Clock signal. (a) Digitized clock waveform. (b) Bandpass filtered clock waveform.

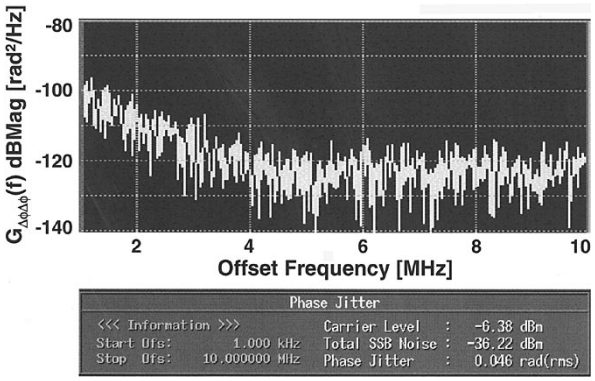

Fig. 19. Phase noise spectrum measured by the phase detector method.

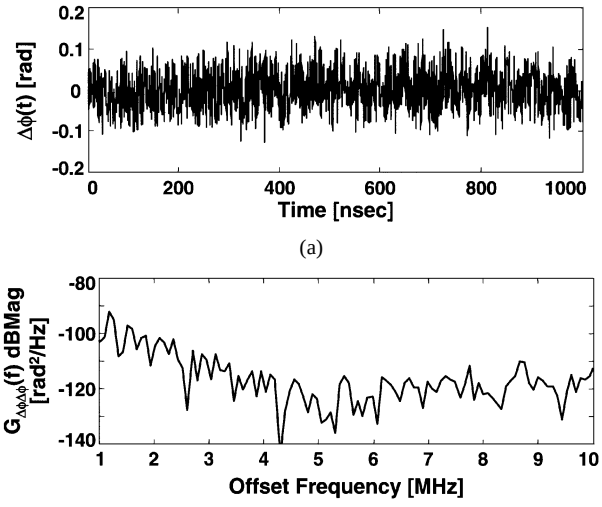

Fig. 20. Phase noise spectrum estimated by the $\Delta\phi$ method. (a) Instantaneous phase noise. (b) Phase noise spectrum.

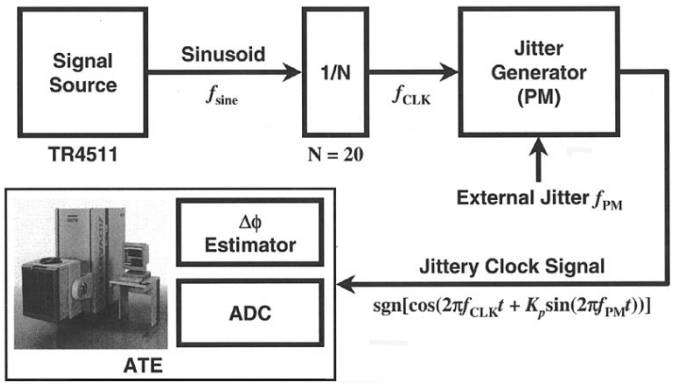

Fig. 21. Experimental setup for validating the $\Delta\phi$ method.

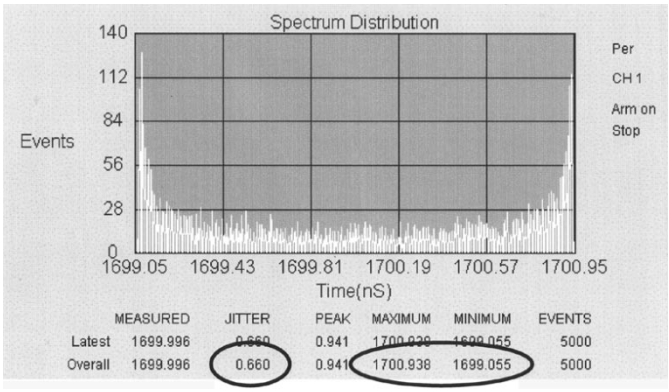

Fig. 22. Jitter histogram estimated using the TIA method.

From this result, it can be seen that the $\Delta\phi$ method is able to estimate the phase noise by oversampling the clock signal at the oversampling ratio (sampling frequency divided by the Nyquist frequency) of at least 2.0. The clock recovery circuit generates a clock of 2.49 GHz by squaring the bit stream being input at 1.24 GHz. With the recovered clock frequency at 2.49 GHz, the Nyquist frequency is 4.98 GHz. The oscilloscope sampling frequency is 10 GHz, thus the oversampling ratio for this specific experiment is 10 GHz/4.98 GHz = 2.01. Since the filtered waveform, illustrated in Fig. 18(b), was sampled at 4 sample points per period, it does not look as smooth as would generally be expected.

In summary, the $\Delta\phi$ method provides $\sigma_{\Delta\phi}$ and $d(\{\Delta\phi\})$ estimates that show excellent agreement with those values estimated by the phase detector method and zero-crossing method, respectively.

VI. Experimental Results Using Sinusoidal Noise Source

In this section experimental measurements of rms and peak-to-peak period jitter (J_{RMS} and J_{PP}) between the $\Delta\phi$ method and the TIA method (Wavecrest DTS 2077) are compared [14]. Sinusoidal noise was used to create controlled jitter. A jitter-free clock signal was divided by 20 and was phase modulated by the sinusoid (Fig. 21). An ATE (Advantest T6682 with built-in 12 bit ADC, $f_{\mathrm{SAMPLING}} = 40.96$ MHz) was used to implement the $\Delta\phi$ method. The sinusoidal jitter signal was analyzed by both methods to extract estimates of jitter values. The total number of samples used was 16 384.

The jitter signal can be written as,

$$\mathrm{sgn}\left[\cos\left(2\pi f_{\mathrm{CLK}}t + K_p \sin\left(2\pi f_{\mathrm{PM}}t\right)\right)\right]$$

where $sgn[\bullet]$ is the signum function, K_p is the maximum phase deviation, $f_{\mathrm{CLK}} = 10$ MHz, and $f_{\mathrm{PM}} = 300$ kHz.

A. Jitter Histogram Comparison

The jitter histogram of the phase modulation signal with $K_p = 1000$ ps (measured by the TIA) is shown in Fig. 22. Note that half the period of the sine wave is used as cycle spacing n between $\Delta\phi[m]$ and $\Delta\phi[m+n]$ in (16). The J_{RMS} value is 660 ps and the J_{PP} value is 1883 ps. Fig. 23 is the corresponding histogram estimated by the $\Delta\phi$ method. It indicates a J_{RMS} value of 650 ps and a J_{PP} value of 1940 ps. The two histograms show the same sinusoidal probability density function.

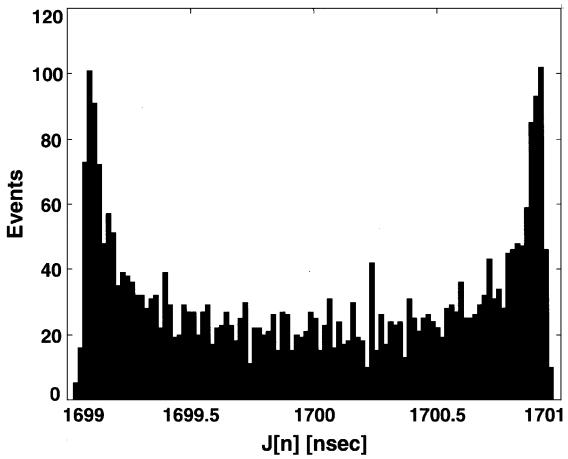

Fig. 23. Period jitter histogram estimated using the $\Delta\phi$ method.

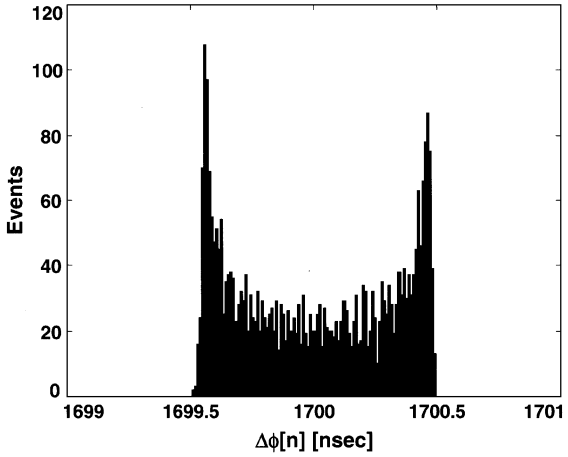

Fig. 24. Timing jitter histogram estimated using the $\Delta\phi$ method.

The histogram of the timing jitter sequence $\Delta\phi[n]$ is shown in Fig. 24. The relationship between J_{RMS} and $\Delta\phi_{\mathrm{RMS}}$, which was predicted by (17), can be validated by comparing the period jitter histogram in Fig. 23 with the timing jitter histogram in Fig. 24. Fig. 25 shows the relationship between the measured jitter ratio and $\rho(n)$, which is estimated from $\{\Delta\phi[m]\}$ by varying nT. The theoretical curve and measured values agree

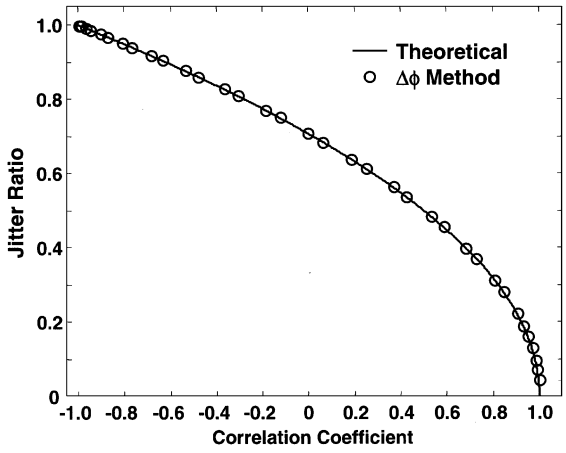

Fig. 25. Jitter ratio and correlation coefficient.

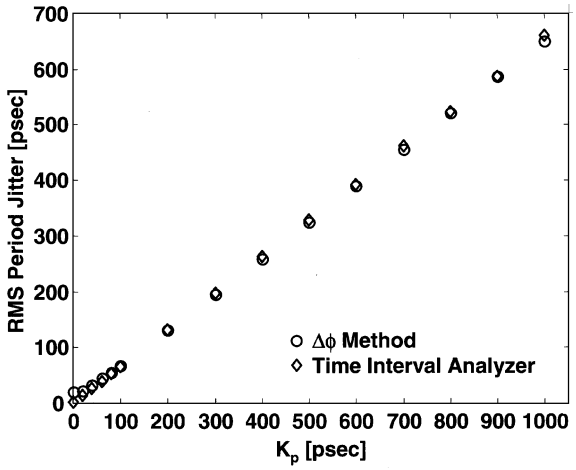

Fig. 26. RMS period jitter measurements for sinusoidal jitter.

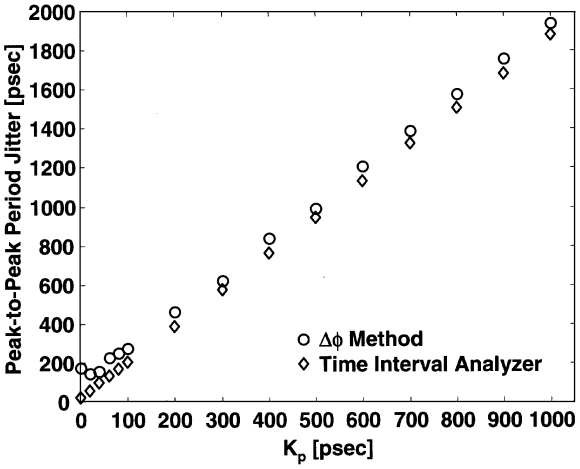

Fig. 27. Peak-to-peak period jitter measurements for sinusoidal jitter.

with each other. Therefore the relationship described by (16) is also validated.

B. Peak-to-Peak Jitter and rms Jitter Estimation

Fig. 26 shows the J_{RMS} estimates as a function of K_p of the sinusoidal phase modulation signal. The diamond symbol corresponds to data measured using the TIA method. It took 2 seconds to collect 5000 zero-crossing events. The symbol "o" indicates J_{RMS} values measured using the $\Delta\phi$ method. It took 0.5 seconds to record 3179 zero-crossing events. The results estimated by the two methods are practically the same. However, the $\Delta\phi$ method requires a much smaller number of zero-crossing events.

Fig. 27 shows J_{PP} estimates as a function of K_p of the sinusoidal phase modulation signal. Both results show linearity with respect to K_p. However, the J_{PP} values estimated by the $\Delta\phi$ method are 3 percent greater than those values estimated with the TIA method. This is due to the limitation of time resolution of the TIA method, which was pointed out in Section IV-B. On the other hand, since the $\Delta\phi$ method can estimate instantaneous phase without using a counter, it does not suffer from the limitation of time resolution.

The accuracy of the method depends on the relative magnitudes of the clock phase noise and the overall system noise. If the system noise is of the same order as the clock phase noise, the jitter measurement accuracy is severely degraded, no matter which method is used. If the system noise is much lower than the clock phase noise, the jitter extraction using the $\Delta\phi$ method is much more accurate.

In summary, the $\Delta\phi$ method provides more accurate estimates of J_{PP} than the TIA method, and requires a shorter measurement time.

VII. Conclusions

An analytic signal method that simultaneously extracts period jitter, timing jitter and phase noise from PLL signals was presented. The new $\Delta\phi$ method employs a combination of the Hilbert transform with a zero-crossing re-sampler. This combination leads directly to a procedure with high throughput, high accuracy, and one that can be implemented in real test applications.

Given a low overall system noise and a sufficient over sampling ratio as discussed above, this method should be optimum for measuring extremely small jitter in PLL signals. The $\Delta\phi$ method does require over sampling of the signal by twice the Nyquist rate. This is not a limitation though, since commercially available ADCs can currently sample at up to 20 GHz.

Acknowledgment

The authors would like to thank H. Oura, CEO of Advantest Corp., T. Maruyama, COO of Advantest Corp., and M. Kamiya, President of Advantest Laboratories Ltd. for their encouragement and support of this research. They also wish to acknowledge the following people for their helpful discussion: S. Sugamori, CTO of Advantest Corporation, and Dr. Y. Maeda, Director of Advantest Laboratories Ltd. Furthermore, the authors would like to thank the anonymous reviewers for their constructive comments, suggestions, and for encouraging them to clarify the advantages of this novel method.

REFERENCES

[1] B. Razavi, "A 2.5-Gb/s 15-mV clock recovery circuit," *IEEE J. Solid-State Circuits*, vol. 31, pp. 472–480, Apr. 1996.

[2] *GR-1377, SONET OC-192 Transport System Generic Criteria*, Bellcore, Issue 5, 1998.

[3] B. Razavi, *Monolithic Phase-Locked Loops and Clock Recovery Circuits: Theory and Design*. New York: IEEE Press, 1996.

[4] ——, "Analysis, modeling, and simulation of phase noise in monolithic voltage-controlled oscillators," in *Proc. IEEE Custom Integrated Circuits Conf.*, 1995, pp. 323–326.

[5] T. C. Weigandt, B. Kim, and P. R. Gray, "Analysis of timing jitter in CMOS ring oscillators," in *Proc. IEEE Int.Symp. on Circuits and Systems*, 1994, pp. 27–30.

[6] B. R. Veillette and G. W. Roberts, "On-Chip measurement of the jitter transfer function of charge-pump phase-locked loops," in *Proc. IEEE Int. Test Conf.*, Washington, DC, 1997, pp. 776–785.

[7] ——, "Stimulus generation for built-in self-test of charge-pump phase-locked loops," in *Proc. IEEE Int. Test Conf.*, Washington, DC, 1998, pp. 698–707.

[8] C. M. Miller and D. J. McQuate, "Jitter analysis of high-speed digital systems," *Hewlett-Packard J.*, pp. 49–56, 1995.

[9] D. Chu, "Phase digitizing sharpens timing measurements," *IEEE Spectrum*, pp. 28–32, July 1988.

[10] J. Wilstrup, "A method of serial data jitter analysis using one-shot time interval measurements," in *Proc. IEEE Int. Test Conf.*, Washington, DC, 1998, pp. 819–823.

[11] A. Papoulis, *Probability, Random Variables, and Stochastic Processes*, 2nd ed. New York: McGraw-Hill, 1984.

[12] J. S. Bendat and A. G. Piersol, *Random Data: Analysis and Measurement Procedure*, 2nd ed. New York: Wiley, 1986.

[13] E. O. Brigham, *The Fast Fourier Transform*. Englewood Cliffs, NJ: Prentice Hall, 1974.

[14] T. J. Yamaguchi, M. Soma, M. Ishida, T. Watanabe, and T. Ohmi, "Extraction of peak-to-peak and RMS sinusoidal jitter using an analytic signal method," in *Proc. IEEE VLSI Test Symp.*, Montreal, Canada, 2000, pp. 395–402.

[15] K. Feher, *Telecommunications Measurements, Analysis, and Instrumentation*. Englewood Cliffs, NJ: Prentice-Hall, 1987.

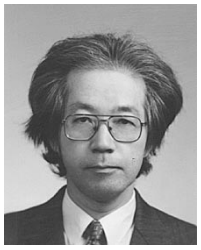

Takahiro J. Yamaguchi (M'85) received the B.S. degree in applied physics from Fukui University, Fukui, Japan, the M.S. degree in physics, and Ph.D. degree in electronic engineering from Tohoku University, Sendai, Japan, in 1976, 1978, and 1999, respectively.

At Advantest Corporation, which he joined in 1978, he was an R&D project manager for Fourier analyzers, FFT-based servo analyzers, Michelson-type optical spectrum analyzers, and TV signal analyzers. He has also contributed to the development of digital signal processing algorithms. Since 1991, he has worked at Advantest Laboratories Ltd., Japan. His research interests are in the application of digital signal processing techniques to testing ADC, DAC, PLL, and SerDes devices as well as data compression methods, and contextual design.

Dr. Yamaguchi is a member of Association for Computing Machinery (ACM) and the Information Processing Society of Japan.

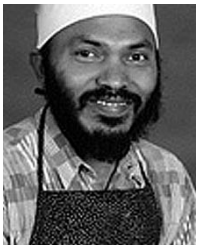

Mani Soma received the B.S.E.E. degree from California State University at Fresno in 1975, and the M.S. and Ph.D. degrees from Stanford University, Stanford, CA, in 1977 and 1980, respectively.

From 1980 to 1982, he was at the General Electric Research and Development Center (Schenectady, NY), working on design and test methodologies for VLSI integrated circuits and systems. He then joined the Department of Electrical Engineering at the University of Washington and has been a Professor since 1988. He was the Associate Director of the NSF Center for Design of Analog-Digital ICs from 1989 to 1994. He has published papers in electronic design, test, and reliability; and has more recently focused on research in mixed analog-digital system design and test.

Dr. Soma founded and chaired the IEEE Mixed-Signal Test Bus Standard Working Group (1149.4) from 1991 to 1995, and remains active in standard development. He was Technical Program Chair for ISCAS 1995 and helped found the Pacific Northwest Test Workshop, which has become the annual IEEE International Mixed-Signal Testing Workshop. For these works, he received the IEEE Computer Society Meritorious Service Award (1995) and the IEEE Computer Society Golden Core Award (1997). He is a Fellow of the IEEE for "contributions to mixed analog-digital system design-for-test."

Masahiro Ishida received the B.S. degree and the M.S. degree in electronic and information engineering from Tokyo University of Agriculture and Technology, Tokyo, Japan, in 1993 and 1995, respectively.

Since 1995, he has worked at Advantest Laboratories Ltd., Japan. His current research interests include test data compression, power supply current testing, and jitter testing.

Toshifumi Watanabe was born in Toyoshina of Nagano, Japan in 1971. He received the B.S. degree and the M.S. degree in applied physics from Waseda University, Tokyo, Japan, in 1994 and 1996, respectively. In 1996, he joined Advantest and currently has been working as a mixed signal application engineer for automatic test equipment. His interests include new test methodologies and system development for testing mixed-signal integrated circuits.

Tadahiro Ohmi received the B.S, M.S. and Ph.D degrees in electrical engineering from Tokyo Institute of Technology, Tokyo, in 1961, 1963, and 1966, respectively.

From 1966 until 1972, Prof. Ohmi served as a research associate in the Department of Electronics, Tokyo Institute of Technology. Then, he moved to Research Institute of Electrical Communication, Tohoku University, Sendai, Japan, and became an associate professor in 1976. In 1985, he became a professor at Department of Electronics, Faculty of Engineering, Tohoku University. Since 1998, he has been a professor at the New Industry Creation Hatchery Center (NICHe), Tohoku University.

His research field covers whole Si-based semiconductor and flat panel display technologies in terms of material, process, device, circuit, and system technologies. He is known as an originator of the "Ultraclean Technology," which introduced ultraclean and the scientific way of thinking into semiconductor manufacturing industry which has become indispensable technology today. He is now promoting the "New Intelligence for IC Differentiation (DIIN)" project at Tohoku University.